AD-A132 881 DIELECTRIC RESONATORS FOR USE IN MICROWAVE AND MILLIMETER-WAVE GAAS CIRCUITS(U) NAVAL RESEARCH LAB WASHINGTON DC 8 E SPIELMAN ET AL. 02 SEP 83 1/1

UNCLASSIFIED NRL-MR-5156 F/G 9/5 NL

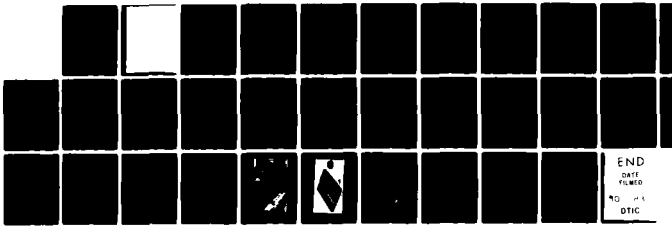

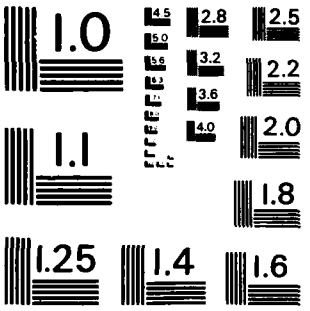

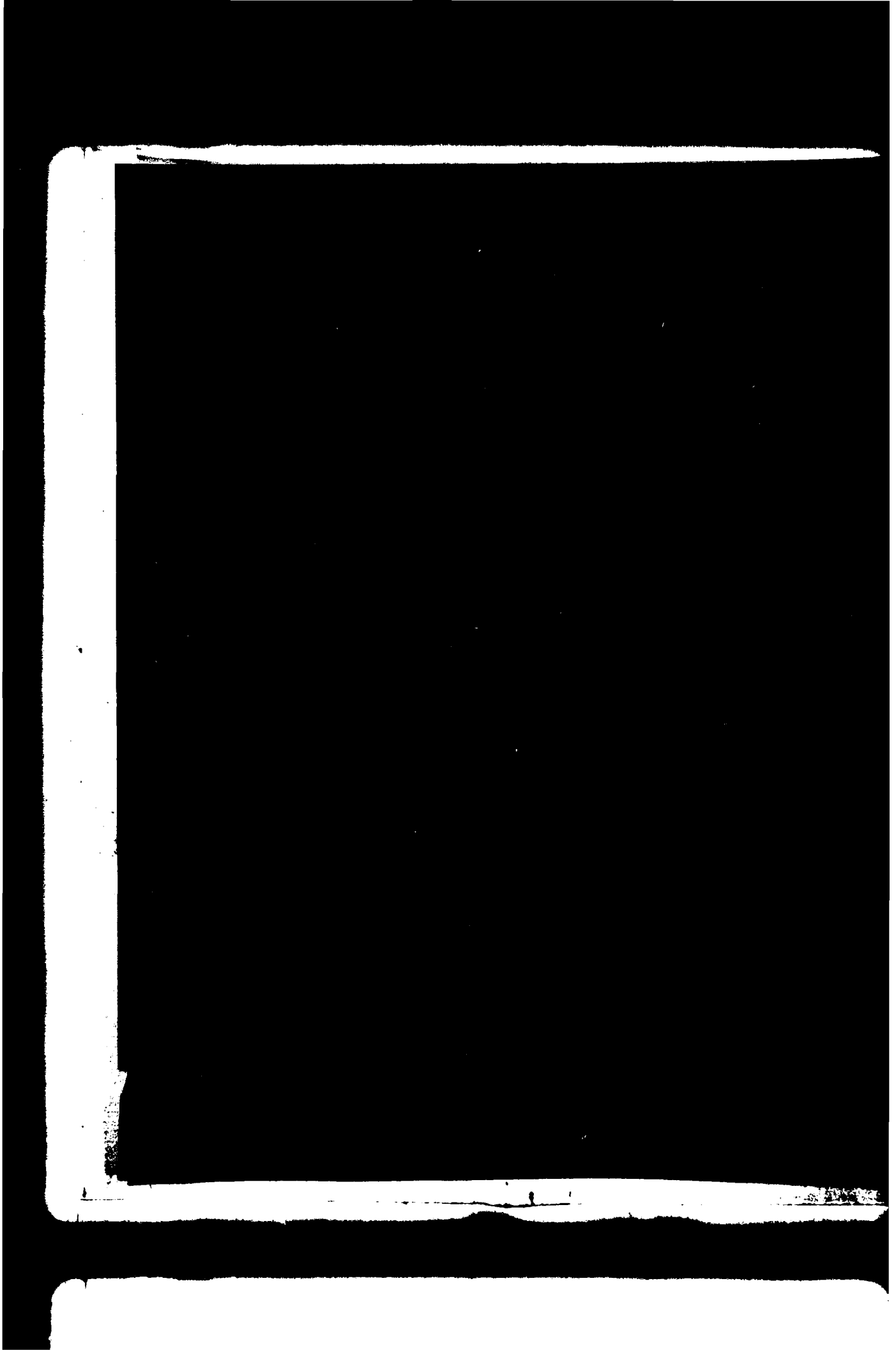

SECURITY CLASSIFICATION OF THIS PAGE (When Data Entered)

REPORT DOCUMENTATION PAGE		READ INSTRUCTIONS BEFORE COMPLETING FORM
1. REPORT NUMBER NRL Memorandum Report 5156	2. GOVT ACCESSION NO. A132 881	3. RECIPIENT'S CATALOG NUMBER
4. TITLE (and Subtitle) DIELECTRIC RESONATORS FOR USE IN MICROWAVE AND MILLIMETER-WAVE GaAs CIRCUITS		5. TYPE OF REPORT & PERIOD COVERED Interim report on a continuing NRL problem. 6. PERFORMING ORG. REPORT NUMBER
7. AUTHOR(s) B.E. Spielman and H.E. Heddings		8. CONTRACT OR GRANT NUMBER(s)
9. PERFORMING ORGANIZATION NAME AND ADDRESS Naval Research Laboratory Washington, DC 20375		10. PROGRAM ELEMENT, PROJECT, TASK AREA & WORK UNIT NUMBERS RR021-03-46; 68-1773-0-3
11. CONTROLLING OFFICE NAME AND ADDRESS		12. REPORT DATE September 2, 1983 13. NUMBER OF PAGES 35
14. MONITORING AGENCY NAME & ADDRESS(if different from Controlling Office)		15. SECURITY CLASS. (of this report) UNCLASSIFIED 15a. DECLASSIFICATION/DOWNGRADING SCHEDULE

16. DISTRIBUTION STATEMENT (of this Report)

Approved for public release; distribution unlimited.

17. DISTRIBUTION STATEMENT (of the abstract entered in Block 20, if different from Report)

18. SUPPLEMENTARY NOTES

19. KEY WORDS (Continue on reverse side if necessary and identify by block number)

Microwave integrated circuits	Dielectric resonators
Monolithic integrated circuits	Transverse resonance solution
Gallium Arsenide	Millimeter-wave integrated circuits

20. ABSTRACT (Continue on reverse side if necessary and identify by block number)

This report represents the results of an investigation of dielectric resonators to be processed in GaAs substrates for application to microwave and millimeter-wave monolithic integrated circuits. Zeroth- and first-order analyses are described. These analyses are applied to dielectric resonator structures to be formed in GaAs substrate material by etching an annular gap in the substrate, thereby effectively

(Continues)

DD FORM 1 JAN 73 1473 EDITION OF 1 NOV 68 IS OBSOLETE
S/N 0102-014-6601

SECURITY CLASSIFICATION OF THIS PAGE (When Data Entered)

20. ABSTRACT (Continued)

leaving a circular cylindrical disc of dielectric material to function as a resonator. Plots of geometric parameter variations with frequency are provided for these resonator structures. Tables are presented to show specific resonant structures for frequency-scaled microwave and non-scaled millimeter-wave resonators. Results are discussed, conclusions drawn, and suggestions for further work set forth.

CONTENTS

Dielectric Resonators for Use in Microwave and Millimeter-Wave GaAs Circuits

1. Background

Dielectric resonators are of considerable interest for use in higher microwave and millimeter-wave frequency stabilization circuits and filtering structures. As frequency increases dissipation losses in conducting materials make microstrip-like circuit elements too lossy (low Q) and metal waveguide structures are expensive to machine. Also, as frequency increases, lumped element structures become difficult to realize and are also low in Q. Although dielectric resonators have been of interest for some time [1,2], little effort has been placed on investigating dielectric resonators which are suitable for processing in monolithic microwave and millimeter-wave circuits. It should be noted that recently, some work has been described [3] for coupling monolithic circuits to non-monolithic dielectric resonators. Since GaAs is a substrate material receiving considerable attention for processing monolithic microwave and millimeter-wave circuits, this report describes the preliminary phase of an investigation into dielectric resonators which might be capable of being processed in or on GaAs to interface with surrounding monolithic circuits.

Manuscript approved June 15, 1983.

2. Theoretical Formulation

The initial dielectric resonator structure considered for use in GaAs circuits is depicted in Fig. 1. Figure 1a shows a perspective sketch of such a resonator, while Fig. 1b shows a cross section through the resonator and defines various parameters associaed with the geometry. It should be noted that H (height of the groove bottom above the lower ground plane) is taken to variable down to H equal to zero, where the dielectric resonator is sitting on the lower ground plane. For a given thickness of GaAs substrate T_s, T and H are related by

$$T_s = T + H \tag{1}$$

The initial concept behind this kind of resonator is to determine if reasonable geometries for use at approximately 95 GHz can be found where the groove could be etched into GaAs by "dry etching" methods (e.g. reactive ion etching).

2.1 No Fringing Fields

In order to estimate the geometries feasible for this structure at 95 GHz an approximate analysis was developed. This analysis employs an approach similar to that used by M. Dydyk [4] for dielectric resonator cylinders placed upon some substrate material (usually different from that of the resonator material) and coupled to a microstrip line. The initial treatment employed for the work in this report approximated the resonator of the type shown in Fig. 1 by assuming that the groove is very wide and thereby enabled the Fig. 1 resonator to be analyzed by the treatment described in [4 and 5]. This solution is based upon a transverse resonance method described in [6]. This approach assumes a magnetic wall at the cylinder boundary and thereby neglects fringing fields. The effects of these fringing fields will be accounted for in a refinement to the analysis as shown later.

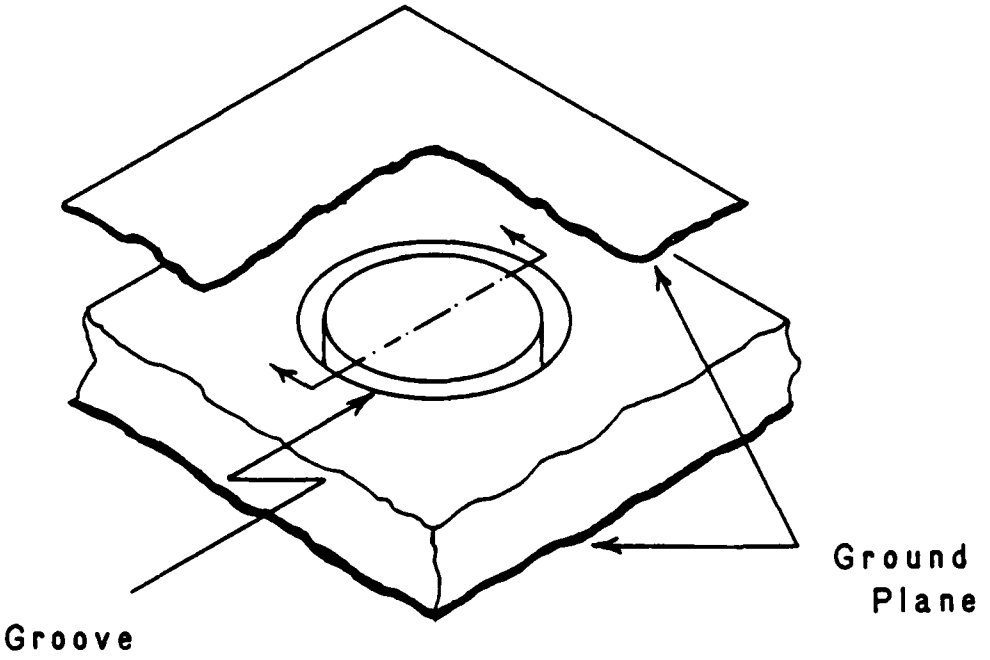

Fig. 1a — Perspective sketch of groove-type dielectric resonator in GaAs.

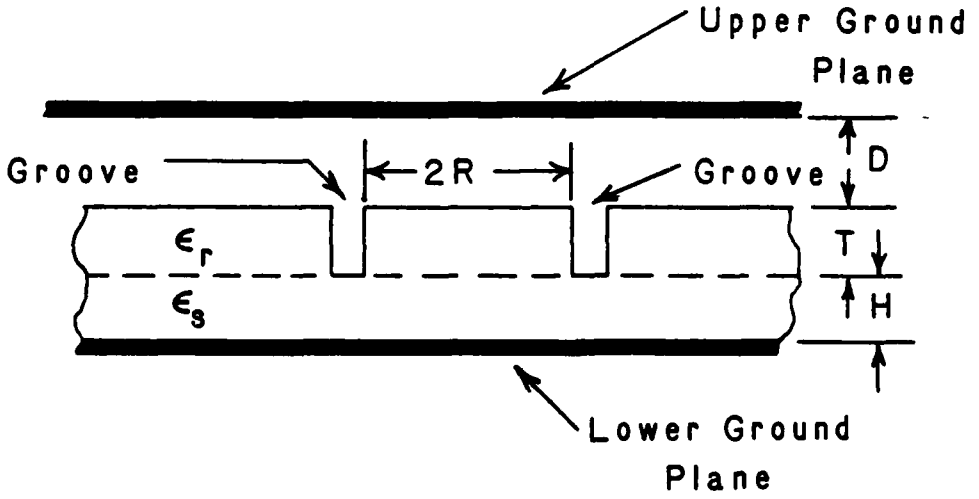

Fig. 1b — Cross section of groove-type dielectric resonator.

For the no fringing case the expression which interrelates the geometry and material parameters for this approximate representation is

$$\frac{T}{2R} = \frac{1}{2\gamma_i R}\left\{\tan^{-1}\left[\frac{\gamma_{oa}R}{\gamma_i R}\coth \gamma_{oa}R\left(\frac{H}{R}\right)\right]\right.$$

$$\left. + \tan^{-1}\left[\frac{\gamma_{os}R}{\gamma_i R}\coth \gamma_{os}R\left(\frac{D}{R}\right)\right]\right\} \quad (2)$$

In (2),

$$\gamma_i = \sqrt{\left(\frac{\omega}{c}\right)^2\varepsilon_r - \left(\frac{2.405}{R}\right)^2} \quad (3)$$

$$\gamma_{oa} = \sqrt{\left(\frac{2.405}{R}\right)^2 - \left(\frac{\omega}{c}\right)^2} \quad (4)$$

$$\gamma_{os} = \sqrt{\left(\frac{2.405}{R}\right)^2 - \left(\frac{\omega}{c}\right)^2\varepsilon_s} \quad (5)$$

Here, c is the velocity of light in free space, ω is the angular frequency of operation, ε_r is the relative permittivity of the cylinder dielectric material, ε_s is the relative permittivity of the substrate and surrounding material on which the cylinder sits. For the special case of the groove-type resonator in GaAs, $\varepsilon_r = \varepsilon_s = 13$. The remaining parameters in equations (2) through (5) are defined in Fig. 1b. Equations (2) through (5) were programmed in general form for digital computer usage. This program is listed and described in Appendix A of this report (see program DRES).

2.2 With Fringing Fields

As described by Dydyk [5], a refinement can be made in the use of equation (2) to account for fringing fields. This is accomplished by solving (6)

$$\beta_{ci}R\left[\frac{J_o(\beta_{ci}R)}{J_1(\beta_{ci}R)}\right] = -\alpha_{co}R\left[\frac{K_o(\alpha_{co}R)}{K_1(\alpha_{co}R)}\right] \quad (6)$$

for $\beta_{ci}R$ and replacing the ratio (2.405/R) in equations (3) through (5) by the newly found β_{ci} value. This process accounts for the decay of fields external to the resonator. In equation (6), J_o is the zeroth order Bessel function of the first kind; J_1 is the first order Bessel function of the first kind; K_o is the zeroth order modified Bessel function of the second kind; and K_1 is the first order modified Bessel function of the second kind. Also in equation (6)

$$\alpha_{co} = \sqrt{\beta^2 - (\frac{\omega}{c})^2} \tag{7}$$

and

$$\beta_{ci} = \sqrt{(\frac{\omega}{c})^2 \varepsilon_r - \beta^2} \tag{8}$$

Solving (6) through (8) to eliminate β yields

$$\beta_{ci}R \left[\frac{J_o(\beta_{ci}R)}{J_1(\beta_{ci}R)} \right] = -Q \left[\frac{K_o(Q)}{K_1(Q)} \right] \tag{9}$$

where $Q = \sqrt{(\frac{R\omega}{c})^2(\varepsilon_r - 1) - (\beta_{ci}R)^2}$. (10)

The solution of equations (9) and (10) were programmed for digital computer usage. This program is listed and described in Appendix B of this report (see program BETACI).

The computer programs listed and described in Appendices A and B were tested for validity by analyzing structures employed by M. Dydyk [4]. In this previous work the solutions were compared to experimental results and were found to agree to within less than two percent error on resonant frequency. Figure 2 shows plots of resonator geometry paramters versus frequency (free space wavelength) for a fixed substrate thickness to radius ratio of H/R = 0.2 with variation in the height of the upper ground plane above the resonator (D/R). Figure 3 shows similar data for the case (D/R) $\rightarrow \infty$ with H/R varying.

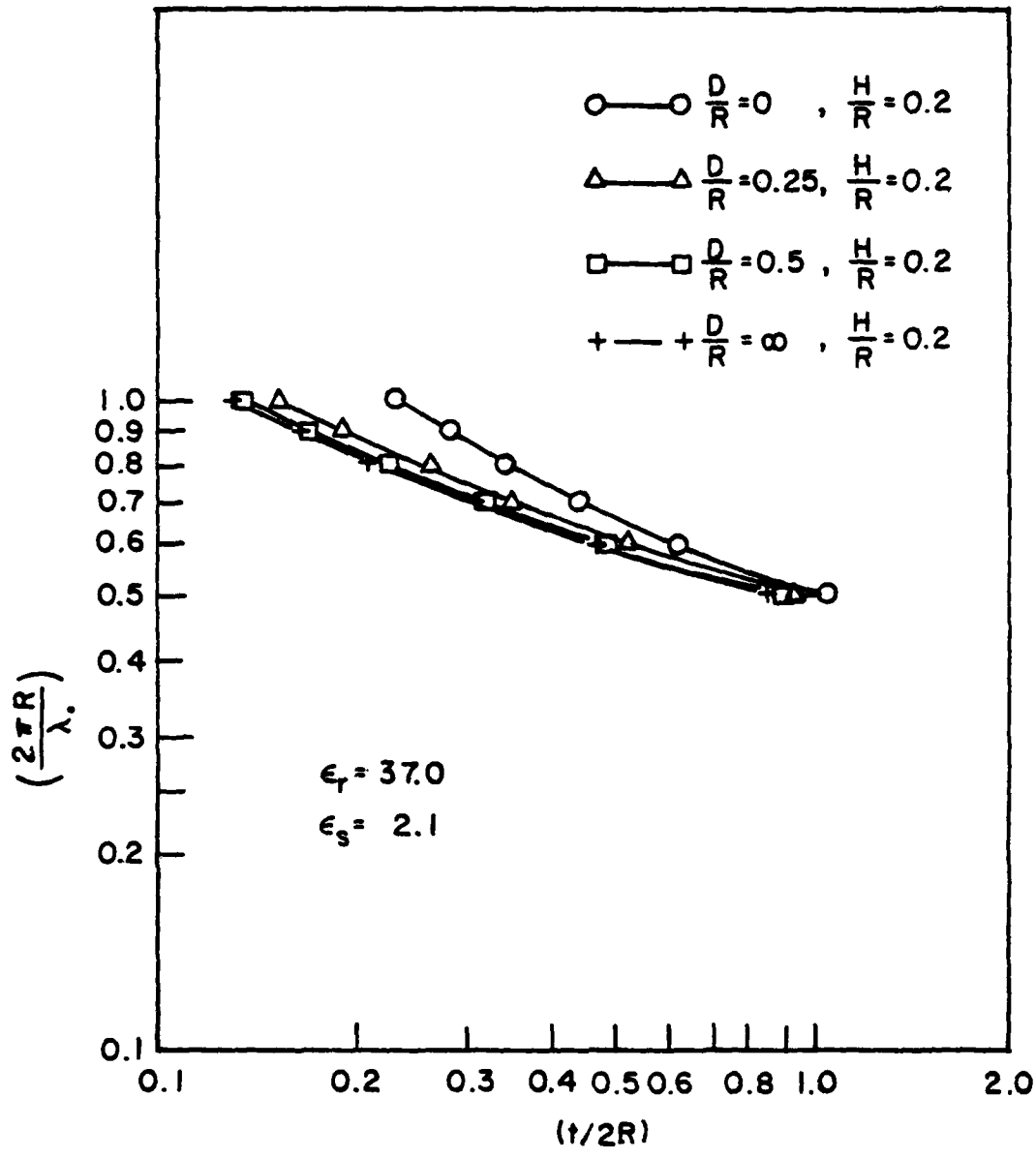

Fig. 2 — Simulation of design geometries for circular disk dielectric resonators on a dielectric substrate for variations in upper ground plane spacing.

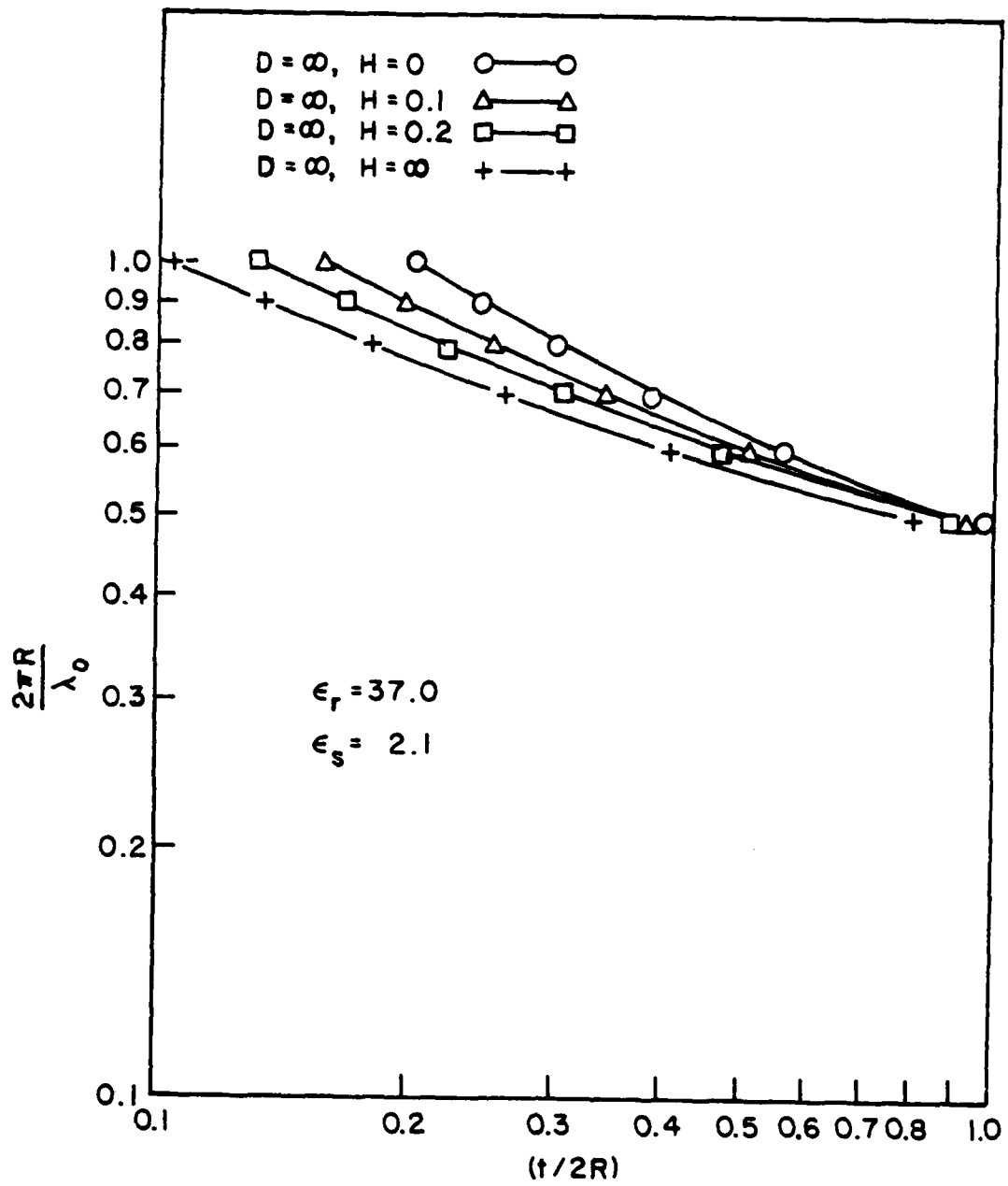

Fig. 3 — Simulation of design geometries for circular disk dielectric resonators on a dielectric substrate for variations in substrate thickness.

For both Figs. 2 and 3 $\varepsilon_r = 37.0$ and $\varepsilon_s = 2.1$. The correlation between Dydyk's results and the results evaluated with the programs used here is extremely close. This close agreement with Dydyk's computational and experimental results has provided verification of the programmed analyses for use on other configurations within the scope of the approximations assumed in treating the groove and coupling mechanism for the resonator.

3. Design Data

The analyses described in section 2, together with implementations shown in Appendices A and B, were applied to the case where $\varepsilon_r = \varepsilon_s = 13$. This case is representative of a resonator and substrate composed completely of semi-insulating GaAs. Figures 4 and 5 display plots of geometry versus frequency for different ranges of resonator thickness T with the upper ground plane sufficiently far removed ($D/R \rightarrow \infty$) so as to have no effect. It was felt that from a practical standpoint this is the most useful case.

From this data it was intended to gather two sets of information. First, design data was to be generated for frequency scaled experiments to investigate coupling mechanism (study the effect of various groove widths) empirically, since this effect is not treated directly by the analyses. Scaled experiments are also necessary to determine the separator necessary between the resonator and microstrip line from which energy is to be coupled. By scaling to lower frequencies (microwave) more accurate measurements could be performed with readily-available automated network analyzers. Secondly, Figures 4 and 5 were to be used to generate designs for millimer-wave resonators to determine the feasibility for geometries in GaAs at these higher frequencies.

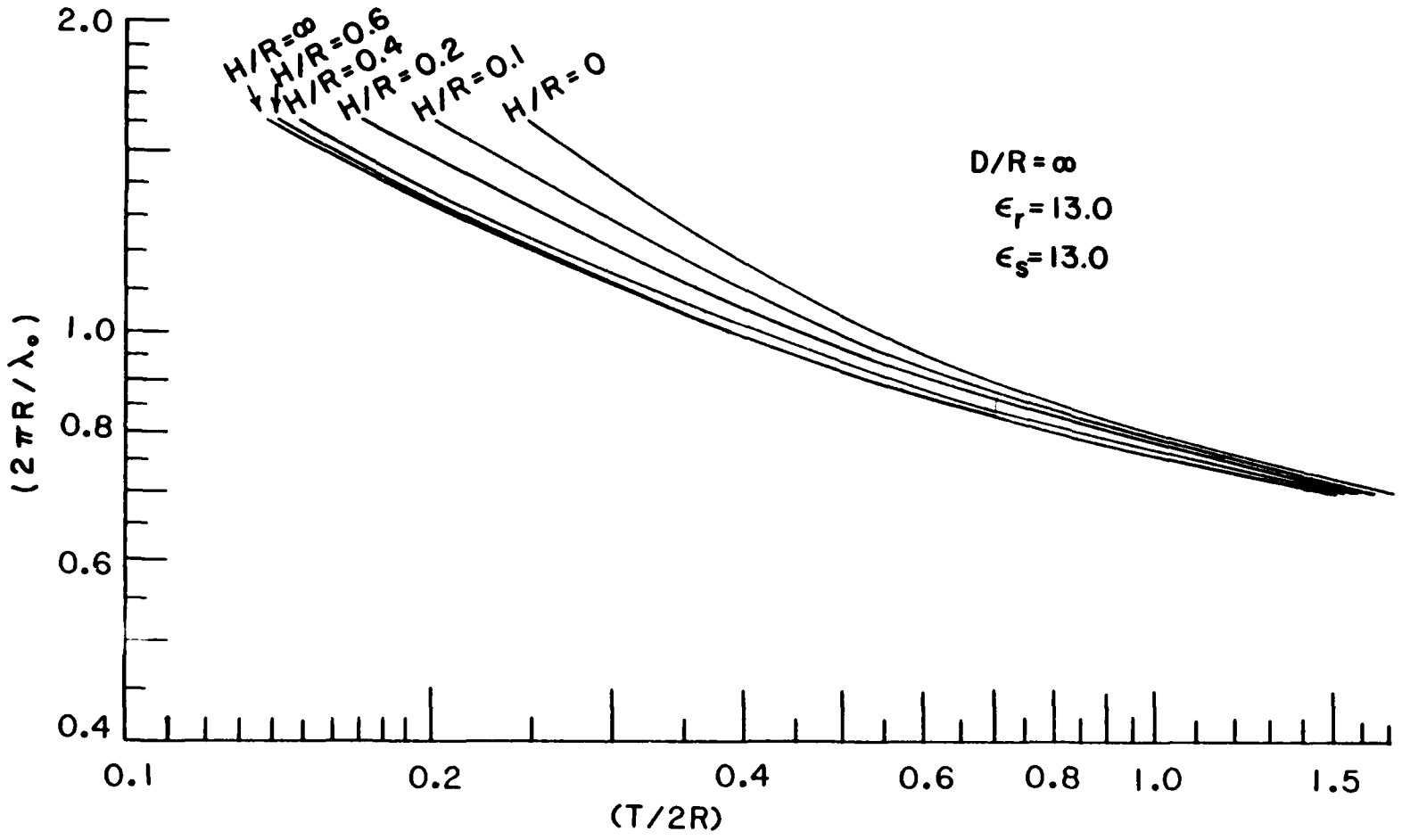

Fig. 4 — Simulation of design geometries for circular disk dielectric (GaAs) resonator on dielectric (GaAs) substrate for variations in substrate height.

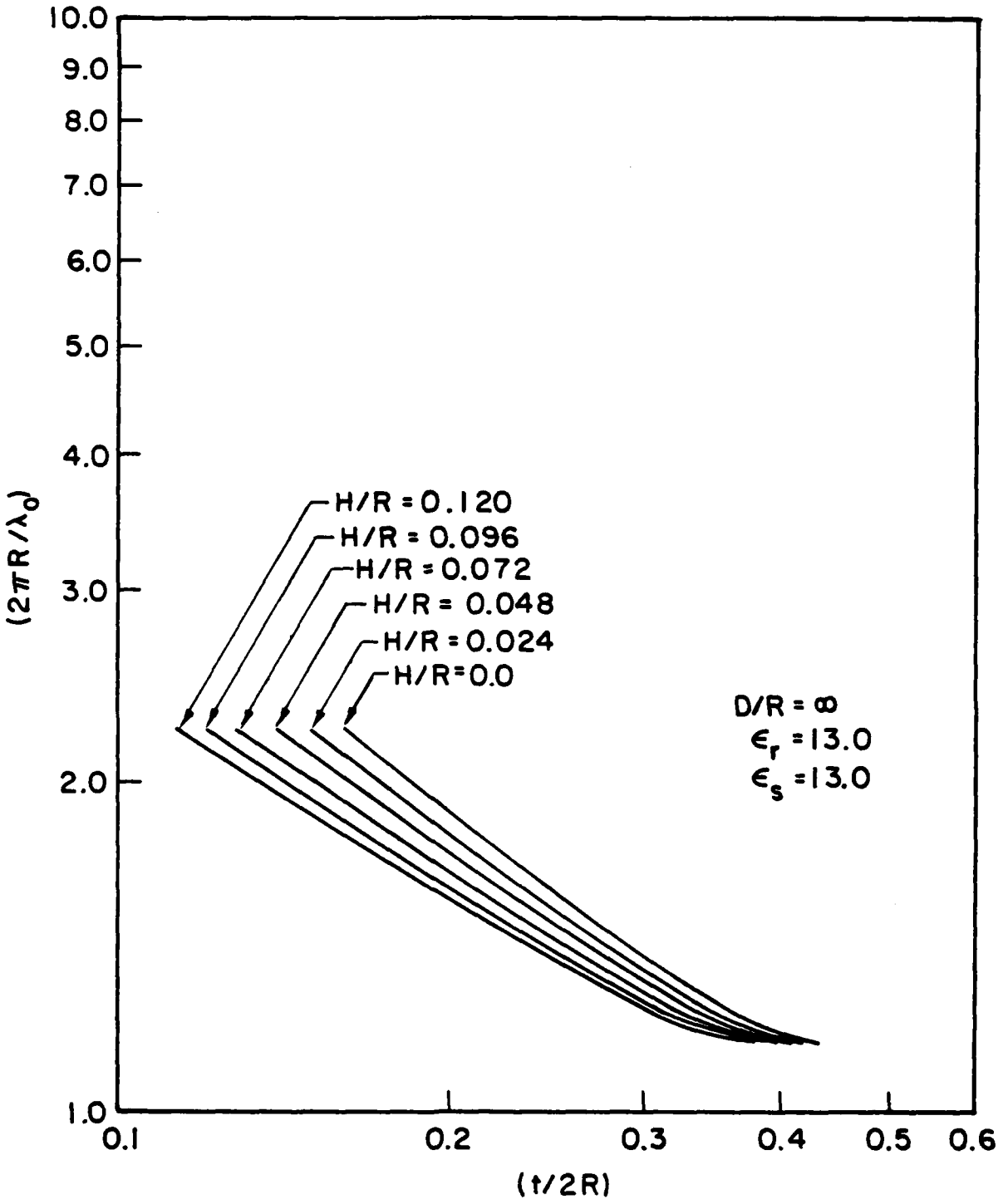

Fig. 5 — Simulation of design geometries for circular disk dielectric (GaAs) resonator on dielectric (GaAs) substrate for this substrates.

The data shown in the following tables was generated to be consistent with several constraints. The data for frequency scaled work (microwave frequencies) was generated for resonances in the 500 MHz to 2 GHz range. For simplification in experiments it was considered desirable to work on TiO_2-loaded Stycast (purchased from Emerson & Cumings, Inc.) sheets having K = 13 and thicknesses of 0.25 inch and 0.50 inch. This would enable: (a) resonator structures to be fabricated by simple machine processes; (b) use of n-type connectors for launching into coupling microstrip lines, and (c) use of metal (e.g. aluminum) foil sheets to be used for simulating the relatively wide microstrip lines needed for use at these frequencies. Further discussion of these experiments will be provided in section 4 of this report.

For $T + H \leq 0.250$ inch, $D \rightarrow \infty$

Table I. (R = 1.25 inch)

(T/2R)	(H/R)	$(2\pi R/\lambda_o)$	T(IN)	H(IN)	$f_o(GH_z)$
0.100	0	3.3	0.250	0.	5.0
0.075	0.05	3.4	0.188	0.062	5.1
0.050	0.10	3.7	0.125	0.125	5.6

Table II. (R = 0.625 inch)

(T/2R)	(H/R)	$(2\pi R/\lambda_o)$	T(IN)	H(IN)	$f_o(GH_z)$
0.2	0.	1.87	0.250	0.	5.6
0.175	0.05	1.88	0.219	0.031	5.7
0.150	0.10	1.92	0.188	0.062	5.8
0.100	0.20	2.2	0.125	0.125	6.6
0.050	0.30	2.8	0.062	0.188	8.4

Table III. (R = 0.3125 inch)

(T/2R)	(H/R)	$(2\pi R/\lambda_o)$	T(IN)	H(IN)	$f_o(GH_z)$
0.400	0.	1.17	0.250	0.	7.0
0.375	0.05	1.17	0.234	0.0156	7.0
0.350	0.10	1.17	0.219	0.0312	7.0
0.300	0.20	1.20	0.188	0.0625	7.2
0.200	0.40	1.37	0.125	0.125	8.2
0.100	0.60	1.9	0.0625	0.188	11.4
0.050	0.70	2.5	0.0312	0.219	15.0

Table IV. (R = 2.50 inch)

(T/2R)	(H/R)	$(2\pi R/\lambda_o)$	T(IN)	H(IN)	$f_o(GH_z)$
0.05	0.	4.2	0.25	0.	3.2

Table IV. (R = 5.0 inch)

(T/2R)	(H/R)	$(2\pi R/\lambda_o)$	T(IN)	H(IN)	$f_o(GH_z)$
0.025	0.	7.3	0.25	0.	2.7

For $T + H \leqq 0.125$ inch, $D/R \rightarrow \infty$

Table V. (R = 0.625 inch)

(T/2R)	(H/R)	$(2\pi R/\lambda_o)$	T(IN)	H(IN)	$f_o(GH_z)$
0.1	0.	3.3	0.125	0.	9.9

Table VI. (R = 0.3125 inch)

(T/2R)	(H/R)	$(2\pi R/\lambda_o)$	T(IN)	H(IN)	$f_o(GH_z)$
0.200	0.	1.88	0.125	0.	11.3
0.175	0.05	2.05	0.109	0.016	12.3
0.150	0.10	2.29	0.094	0.031	13.8
0.100	0.20	3.00	0.032	0.063	18.0

Table VII. (R = 0.15625 inch)

(T/2R)	(H/R)	$(2\pi R/\lambda_o)$	T(IN)	H(IN)	$f_o(GH_z)$
0.400	0.	1.17	0.125	0.	14.1
0.375	0.05	1.17	0.117	0.008	14.1
0.350	0.10	1.17	0.109	0.016	14.1
0.300	0.20	1.20	0.094	0.031	14.4
0.250	0.30	1.27	0.078	0.047	15.3
0.200	0.40	1.37	0.062	0.063	16.5
0.150	0.50	1.57	0.047	0.078	18.9
0.100	0.60	1.90	0.032	0.093	22.8

For millimeter-wave operation in the vicinity of 100 GHz, the following tables provide results of interest. For $T + H \leq 0.002$ inch

Table VIII. (R = 0.004 inch)

(T/2R)	(H/R)	$(2\pi R/\lambda_o)$	T(IN)	H(IN)	$f_o(GH_z)$
0.250	0.	1.57	0.00200	0.	738.
0.225	0.05	1.59	0.00180	0.0002	747.
0.200	0.10	1.60	0.00160	0.0004	752.
0.150	0.20	1.73	0.00120	0.0008	813.

Table IX.

(T/2R)	(H/R)	$(2\pi R/\lambda_o)$	T(IN)	H(IN)	T+H(IN)	R(IN)	$f_o(GH_z)$
0.250	0.	1.57	0.014760	0.	0.014760	0.02952	100.
0.225	0.05	1.58	0.013446	0.001494	0.014940	0.02988	99.4
0.200	0.10	1.60	0.012032	0.003008	0.015140	0.03008	100.
0.150	0.20	1.73	0.009756	0.006504	0.016260	0.03252	100.
0.113	0.12	2.23	0.009469	0.005028	0.014497	0.04190	100.

Table X.

(T/2R)	(H/R)	$(2\pi R/\lambda_o)$	T(IN)	H(IN)	T+H(IN)	R(IN)	$f_o(GH_z)$
0.025	0.0	6.9	0.00648	0.	0.00648	0.1296	100.
0.010	0.0	13.5	0.00508	0.	0.00508	0.2540	99.9
0.005	0.0	21.4	0.00402	0.	0.00402	0.4020	100.
0.00167	0.0	44.5	0.00278	0.	0.00278	0.8340	100.

4. Discussion and Conclusions

The data plotted in Figs. 4 and 5 were generated to simulate dielectric resonators formed in GaAs substrates. For these data the height of the upper ground plane above the resonator structure (see Figs. 1a and 1b) was taken to be sufficiently large so that the influence of the ground plane on the circuit performance would be insignificant. This height was determined by evaluating performance for several different height values for each resonant structure to determine that height value for which the interaction becomes insignificant with regard to influencing the first three significant figures in computed values of T/2R.

The data plotted in these figures is applicable to resonators operating at frequencies occurring from the microwave through the millimeter-wave regime. It should be noted that, although the analyses described in this report were developed to be invoked for groove-type resonators (with wide groove approximation), they are applicable to and even more accurate for all GaAs resonator/substrate combinations where a circular-cylindrical disk resides on a substrate (i.e. no grooves). In addition to the information contained in Figs. 4 and 5, Tables I through VII can be useful for microwave designs of such structures. Tables VIII through X are similarly useful for millimeter-wave realizations.

Once the analyses described in section 2 of this report were operational the investigation of groove-type resonators became one of satisfying the following conditions. In order to accurately characterize resonators including coupling effects associated with the groove and microstrip feed line interactions, reasonable (not too large or too small) geometries needed to be determined to enable experiments to be performed at microwave frquencies where

automated equipment could enable accurate comprehensive resonator characterization. Furthermore, fabrication of versatile test samples is simplified at microwave frequencies due to the larger physical size required, thereby enabling less expensive empirical work to be conducted. On the other hand, when models are scaled for operation at 95 to 100 GHz, the geometries must be compatible with processes employed in monolithic circuit work.

Based upon the data provided in Tables I through X, the following observations were made. In order to fabricate scaled (microwave) model resonators in K=13 material having resonant frequencies below 2 GHz, excessively large diameter resonators are needed (diameters in excess of 10 inches). Furthermore, by virtue of the resonant frequency being affected by both resonator diameter and thickness, it is observed that for 100 GHz geometries (Tables IX and X) that either: excessively large resonator diameters are needed for GaAs substrates which are then enough to make for practical reactive ion etching of annular grooves (e.g. 0.168 inch diameter, 0.0056 inch thick substrate; or excessively thick substrates for practical reactive ion etching of grooves with reasonable rsonator diameters (e.g. 0.0149 inch thickness, 0.030 inch diameter). Additionally, for 100 GHz resonators the coupling microstrip line used to launch energy to the resonator is estimated to require a GaAs substrate thickness of no more than 0.0027 to 0.005 inch (see Appendix C) in order to remain free of higher order mode propagation. For all of these reasons it is felt that other alternatives to dielectric resonator structures with potential compatibility for monolithic realization should be pursued at this point, instead of the groove-type resonator described here. Some alternatives will be described in section 5. It should be noted that since the alternatives to be considered in section 5 do not require groove-type processing, the microwave experiments needed to empirically assess the effects

of the resonator groove are no longer needed. Appendix C describes some preliminary work performed in support of the previously anticipated scaled experimental efforts. Hence, the effects attributable to the "wide groove" approximation are no longer needed.

5. Suggestions for Future Work

For the reasons discussed in the previous section, two categories of dielectric resonators should be considered. One category encompasses the formation of resonators on GaAs substrates by processing layers of higher dielectric constant materal (e.g. Barium titanates) on the substrate surface. The higher dielectric constant material should reduce the geometries needed to achieve mm-wave resonance. The analyses described in section 2 of this report are flexible enough to directly treat such structures. However, significant effort is necessary to study the processing methods needed for realizations. A variation of this approach is to sandwich a lower dielectric constant layer (e.g. k=2 to 4) between the Barium titanate and substrate. This could raise the Q.

A second category of dielectric resonator which might warrant further consideration is the processing of K=13 material on GaAs substrates. The processing methods and material choices need further consideration and analysis. This category is not currently considered as promising as the type mentioned in the preceding paragraph because the geometry reduction is not inherent in these structures. A potential advantage might be accrued, however, in eliminating the need for dry etching thick materials.

APPENDIX A - Program DRES

Program DRES, which computes the characteristics of dielectric circular cylindrical resonators (Figs. 1a and 1b) without fringing is written in FORTRAN IV and is compatible with the CDC CYBER 175 digital computer system. With minor modifications this program should also be suitable for use with digital computer accepting FORTRAN IV encoded programs. Although a precise determination of the execution time of programs has not been determined, experience has shown that a few seconds are needed to determine enough geometric parameters for several frequency points to enable plots of the type shown in Figs. 2 through 5 to be made.

This program embodies the analyses described in section 2.1. When the proper input paramters are specific this program evaluates the ratio T/2R (see Figs. 2 through 5) for given values of $2\pi R/\lambda_o$, H/R, D/R, substrate dielectric constant, and resonator dielectric constant. The input parameters required are described as follows:

ER = relative permittivity of the resonator dielectric material

ES = relative permittivity of the substrate dielectric material

F1 = lowest frequency at which computations are to be performed in GHz

F2 = highest frequency at which computations are to be performed in GHz

NK = number of frequency intervals between F1 and F2 to be used in computations

R = radius of dielectric resonator to be evaluated in inches

The output parameters provided by this program are described as follows:

A = evaluated ratio T/2R

TWOPDL = ratio $2\pi R/\lambda_o$

D = ratio H/R

F = ratio D/R

The following should be taken into consideration if modifications to the program coding are desired. Lines number 00310, 00320, and 00330 are used to set the initial value (-0.024) of the height "H," the number of steps (11) to be taken for incrementing the initial value of "H," and the size of the step (0.025) for "H." Note that in line number 00330 the first computed value for D is 0.001. This is to circumvent problems of singular behavior incurred for D=0.

The listing for program DRES follows.

```
00100 PROGRAM DRES(INPUT,OUTPUT)
00110 PRINT 1
00120 1FORMAT(1H ,*EP,ES,F1,F2,NK,R*)
00150 READ*,EP,ES,F1,F2,NK,R
00151 F1=F1*1.E+09
00152 F2=F2*1.E+09
00153 R=2.54E-02*R
00160 CSPEED=3.0E+08
00170 FACT1=(2.*3.14159)/CSPEED
00180 FACT2R=(2.405*2.405)/(R*R)
00190 FACT12=FACT1*FACT1
00200 DELF=(F2-F1)/10.
00210 FREQI=F1-DELF
00220 DO 2 I=1,11
00230 FREQ=FREQI+DELF
00240 FREQ2=FREQ*FREQ
00250 BARG=FACT12*FREQ2*EP-FACT2R
00251 BARG=ABS(BARG)
00260 B=SQRT(BARG)
00261 B=R*B
00270 CARG=FACT2R-FACT12*FREQ2
00271 CARG=ABS(CARG)
00280 C=SQRT(CARG)
00281 C=R*C
00290 EARG=FACT2R-FACT12*FREQ2*ES
00291 EARG=ABS(EARG)
00300 E=SQRT(EARG)
00301 E=R*E
00310 DI=-0.024
00320 DO 3 J=1,11
00330 D=DI+0.025
00331 D=D*2.54E-02/R
00340 FI=-0.249
00350 DO 4 K=1,NK
00360 F=FI+0.25
00361 F=F*2.54E-02/R
00370 CD=C*D
00380 EF=E*F
00390 HTAN1=TANH(CD)
00400 HCTN1=1./HTAN1
00410 HTAN2=TANH(EF)
00420 HCTN2=1./HTAN2
00430 ATARG1=(C/B)*HCTN1
00440 ATARG2=(E/B)*HCTN2
00450 A=(1./(2.*B))*(ATAN(ATARG1)+ATAN(ATARG2))
00460 TWOPDL=FACT1*FREQ*P
00470 PRINT 5,A,TWOPDL,D,F
00480 5FORMAT(1H ,2HA=,F7.3,3X,7HTWOPDL=,F7.3,3X,2HH=,F7.3,3X,2HD=,F7.3)
00490 FI=F*R/2.54E-02
00500 4CONTINUE
00510 DI=D*R/2.54E-02
00520 3CONTINUE
00530 FREQI=FREQ
00540 2CONTINUE
00550 STOP
00560 END
READY.
```

APPENDIX B - Program BETACI

Program BETACI is written to determine the value of β_{ci}, as described in section 2.2, so that it can be used in program DRES for taking into account fringing field effects of the dielectric resonator behavior. Accessed by program BETACI, but not listed here, are four subroutines available from the Control Data Corporation, Cybernet Services, International Mathematical and Statistical Library (IMSL). These subroutines are named: MMBSJ0, MMBSJ1, MMBSK0, and MMBSK1. MMBSJ0 computes values of the Bessel function of the first kind of order zero. MMBSJ1 computes values of the Bessel function of the first kind order one. MMBSK0 computes values of the modified Bessel function of the second kind of order zero. MMBSK1 computes values of the modified Bessel function of the second kind of order one.

The input parameters for this program are described as follows:

FREQ = frequency to be used in evaluation in hertz

ER = relative permittivity of the dielectric resonator material

BETA = initial estime to be used in search routine to determine β_{ci} (see explanation to follow)

R = radius of resonator in inches

To determine a value of BETA to serve as an input parameter consider the following. Since the argument needed for square root computations (e.g. line number 00210) must be non-negative, then

$$R^2(\frac{2\pi}{c})^2 (\varepsilon_r-1)f^2 - (\beta_{ci}R)^2 \geq 0$$

This means that

$$R^2 \geq \frac{(\beta_{ci}R)^2}{(\frac{2\pi}{c})^2 (\varepsilon_r-1)f^2}$$

Let $R_{3.82}$ be defined by

$$(R_{3.82})^2 = \frac{(3.82)^2}{(\frac{2\pi}{c})^2(\varepsilon_r - 1)f^2}$$

Let the input parameter BETA be determined by

$$\text{BETA} = \frac{2.405}{R_{3.82}}$$

This assures that the argument for certain roots in program BETACI are positive with $\beta_{ci}R$ occurring for the range from 2.405 to 3.82 (the first non-trivial roots for J_0 and J_1, respectively.

Upon receiving the input parameters program BETACI employs a Newton-Raphson method to converge to a value of β_{ci} with accuracy to four significant figures based on the convergence criterion used in line number 00340.

The output quantities provided by program BETACI are described as follows:

BETAR = last value of produce $\beta_{ci}R$ determined in the search process

BETAPR = the last value of $\beta_{ci}R$ determined in the search process but increased by 1/100% for use in finite difference approximations employed in convergence procedure

IERJ0 = output error parameter determined in routine MMBSJ0 (see IMSL writeup on MMBSJ0)

IERJ1 = output error parameter determined in routine MMBSJ1 (see IMSL writeup on MMBSJ1)

IERK0 = output error parameter determined in routine MMBSK0 (see IMSL writeup on MMBSK0)

IERK1 = output error parameter determined in routine MMBSK1 (see IMSL writeup on MMBSK1)

XNUM = numerator used in evaluating increment of $\beta_{ci}R$ for Newton-Raphson method

XDEN = intermediate quantity used for debugging (currently superfluous)

XDENOM = denominator used in evaluating increment of $\beta_{ci}R$ for Newton-Raphson method

It should be noted that all of the above output parameters are used for observing convergence behavior and are typically not necessary as output quantities for normal convergence. IERJ0, IERJ1, IERK0, and IERK1 are equal to zero for properly convergent operation.

Finally,

BETCAL = calculated end value of β_{ci} needed for use with program DRES in $(\text{meters})^{-1}$

Once BETCAL is determined from program BETACI, this value is then used in program DRES for the same parameters by placing line number 00180 in program DRES with "00180 FACT2R = BETCAL*BETCAL." Here, the actual value of BETCAL would be used in lieu of the name BETCAL.

The listing for program BETACI follows.

```
00100 PROGRAM BETACI(INPUT,OUTPUT)
00103 REAL MMBSJ0,MMBSJ1,MMBSK0,MMBSK1
00105 CALL IMSL
00110 PRINT 1
00120 1FORMAT(1H ,4FREQ,EP,BETA,R4)
00130 READ4,FREQ,EP,BETA,R
00140 R=R*2.54E-02
00141 BETAR=BETA*R
00150 IOPT=1
00170 FACT1=(2.*3.14159/3.E+08)*(2.*3.14159/3.E+08)
00181 BETARR=1.0001*BETAR
00182 2IF(BETARR.GE.3.83)4,5
00183 4PRINT 6
00184 6FORMAT(1H ,4BETAR AND BETARR TOO LARGE4)
00185 GO TO 3
00190 5XJ0=MMBSJ0(BETAR,IERJ0)
00191 XJ0R=MMBSJ0(BETARR,IERJ0)
00200 XJ1=MMBSJ1(BETAR,IERJ1)
00201 XJ1R=MMBSJ1(BETARR,IERJ1)
00210 UARG=(R*R*FACT1*(EP-1.)*FREQ*FREQ)-(BETAR*BETAR)
00211 UARGR=(R*R*FACT1*(EP-1.)*FREQ*FREQ)-(BETARR*BETARR)
00220 U=SQRT(UARG)
00221 UR=SQRT(UARGR)
00230 XK0=MMBSK0(IOPT,U,IERK0)
00231 XK0R=MMBSK0(IOPT,UR,IERK0)
00240 XK1=MMBSK1(IOPT,U,IERK1)
00241 XK1R=MMBSK1(IOPT,UR,IERK1)
00250 XNUM=(BETAR*(XJ0/XJ1))+(U*(XK0/XK1))
00251 XNUMR=(BETARR*(XJ0R/XJ1R))+(UR*(XK0R/XK1R))
00260 T1=XJ0/XJ1
00270 T2=BETAR*(((XJ0/XJ1)*(1./BETAR))-((XJ0/XJ1)**2.))
00280 T3=2.*(BETAR/U)*(XK0/XK1)
00290 T4=BETAR*((XK0/XK1)**2.)
00300 XDEN=T1+T2-T3+T4
00301 XDENOM=(XNUMR-XNUM)/(BETARR-BETAR)
00310 H=-XNUM/XDENOM
00315 AH=ABS(H)
00320 BETAR=BETAR+H
00321 BETARR=1.0001*BETAR
00330 PRINT*,BETAR,BETARR,IERJ0,IERJ1,IERK0,IERK1,XNUM,XDEN,XDENOM
00331 BETCAL=BETAR/R
00332 PRINT*,BETCAL
00340 IF(AH.LT.1.E-04)3,2
00350 3STOP
00360 END
READY.
```

APPENDIX C - Preliminary Work for Experiments

The data listed in Tables I through VII were evaluated to provide information needed for guiding geometries to be used in experiments frequency scaled to microwave frequencies where automated equipment could enable accurate, comprehensive resonator characterization. It was initially envisioned that experimental realizations such as those shown in Figs. 6, 7, and 8 could be used. Figure 6 shows a "groove-type" resonator fabricated in TiO_2-loaded stycast with a microstrip line coupled to the resonator. The rf signal is launched and measured through N-type coaxial connectors as shown in Fig. 6. In Fig. 6 the top ground plane is removed to expose the circuit nature. Figure 7 shows the two parts used to form the resonator-circuit structures. The plug seen in this figure is machined as well as the counter-bored hole in the substrate, into which the plug is set and affixed with Emerson and Cuming stycast loaded epoxy having a dielectric constant of 13 to match the dielectric constant of the stycast *board.* The microstrip line and transitions to N-type coaxial connectors were optimized for match on these boards using a Hewlett Packard 1815A time-domain reflectometer. The assembly ultimately used in early experiments employed an upper ground plane and is shown in Fig. 8.

Preliminary measurements were needed on isolated microstrip lines fabricated on stycast boards to ensure that connectors, transitions, and microstrip lines were functioning adequately up to 2 or 3 GHz. Initial measurements were performed using stycast boards (k=13) having a thickness of ½ inch. However, measurements showed that reasonable transition performance for straight through microstrip lines could not be maintained above about 1.2 to 1.5 GHz. Upon making similar measurements using ¼ inch thick stycast boards it was found that adequate performance could be achieved to above 2 GHz. Figures 9 and 10 show the insertion loss and VSWR measurements performed on the ¼ inch

thick board. The limitation on substrate thickness observed by comparing ½ inch thick to ¼ inch thick board results is attributed to that frequency at which higher order modes are launched in the microstrip line.

Prior to that point in time that accurate analyses were ready for use, gross approximations were used to estimate geometries for experimental models so that coupling effects could be studied. It was found that appropriate resonator geometries were not well estimated which resulted in resonators not having detectable resonant frequencies in the frequency range capable of being measured. Once the analyses described in section 2 of this report were operational the problems encountered in early experiments were better understood.

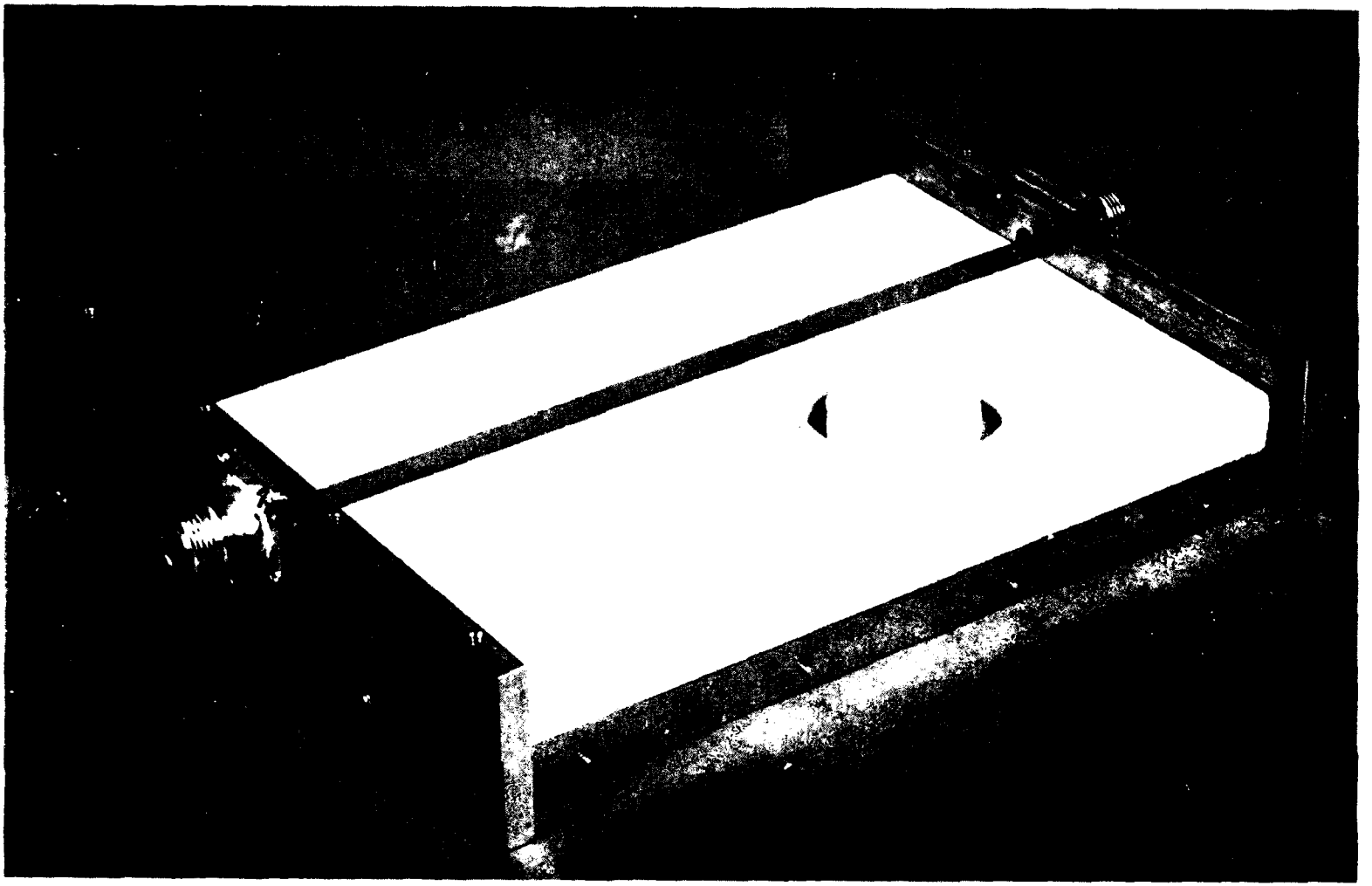

80274(2)

Fig. 6 — Photograph of groove-type dielectric resonator coupled to microstrip line fabricated in k = 13 Stycast material.

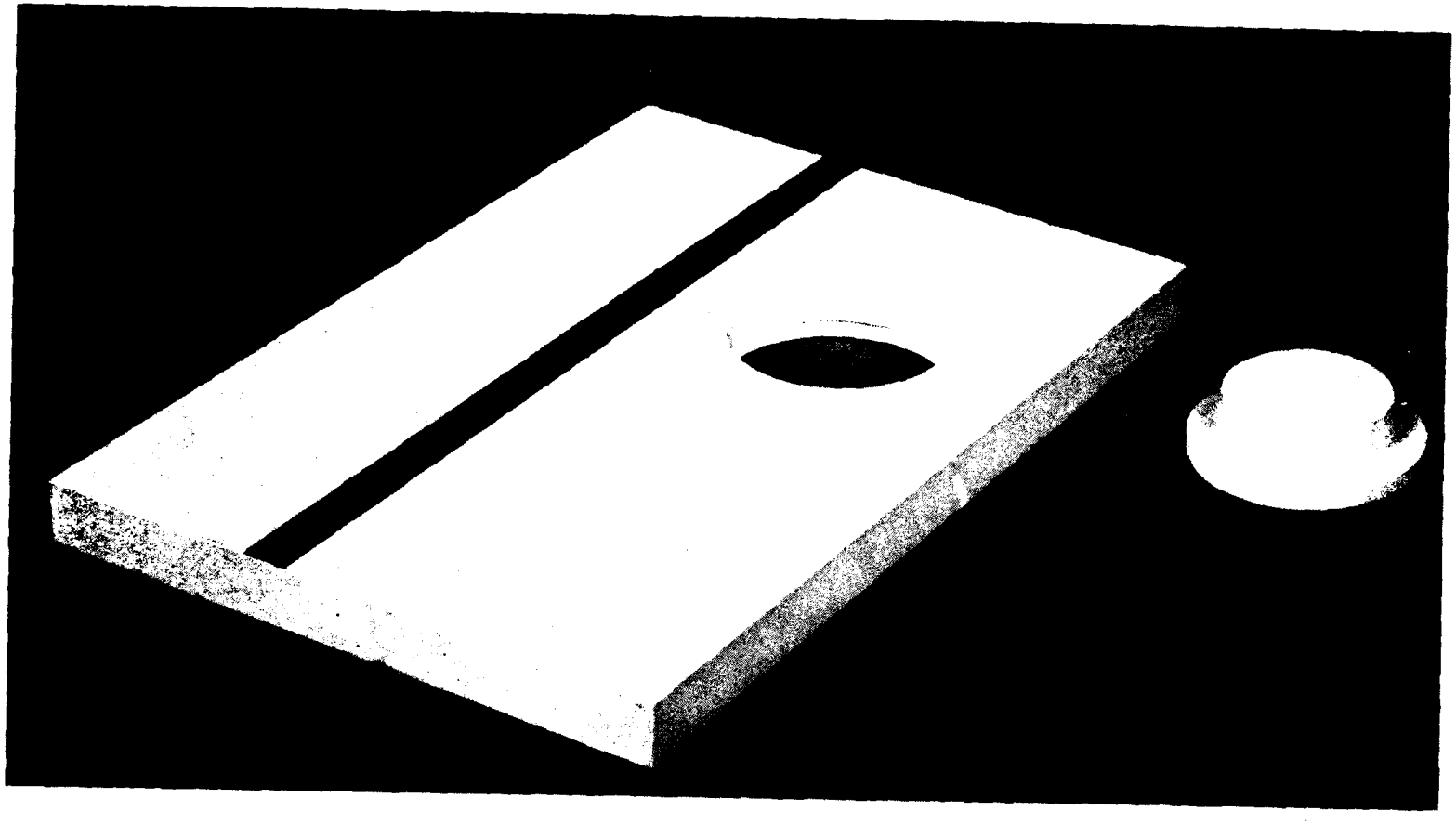

80274(1)

Fig. 7 — Photograph showing dielectric plug and machined board used in Figure 6 assembly.

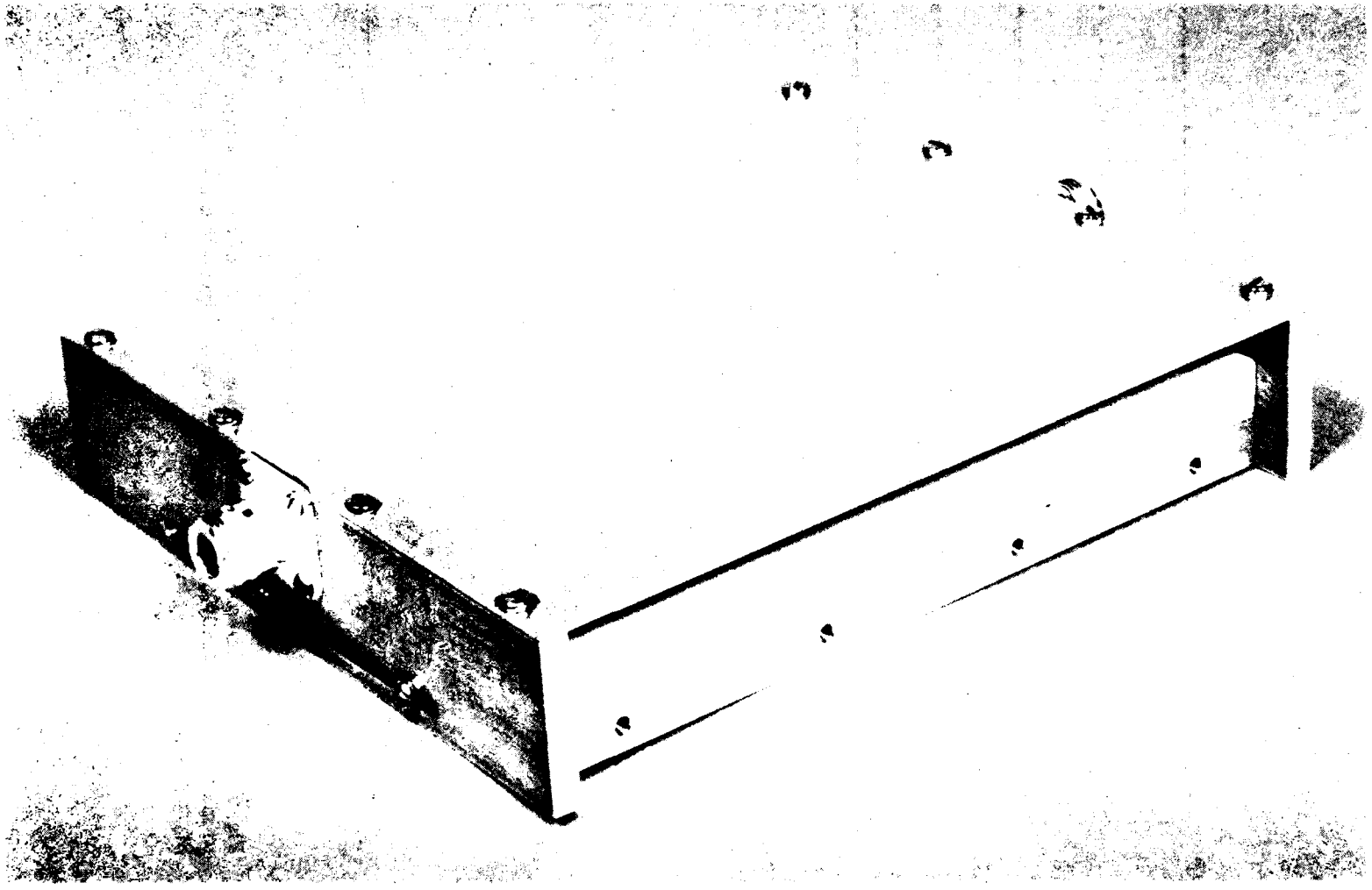

80274(5)

Fig. 8 — Photograph showing Figure 6 assembly with mounted upper ground plane.

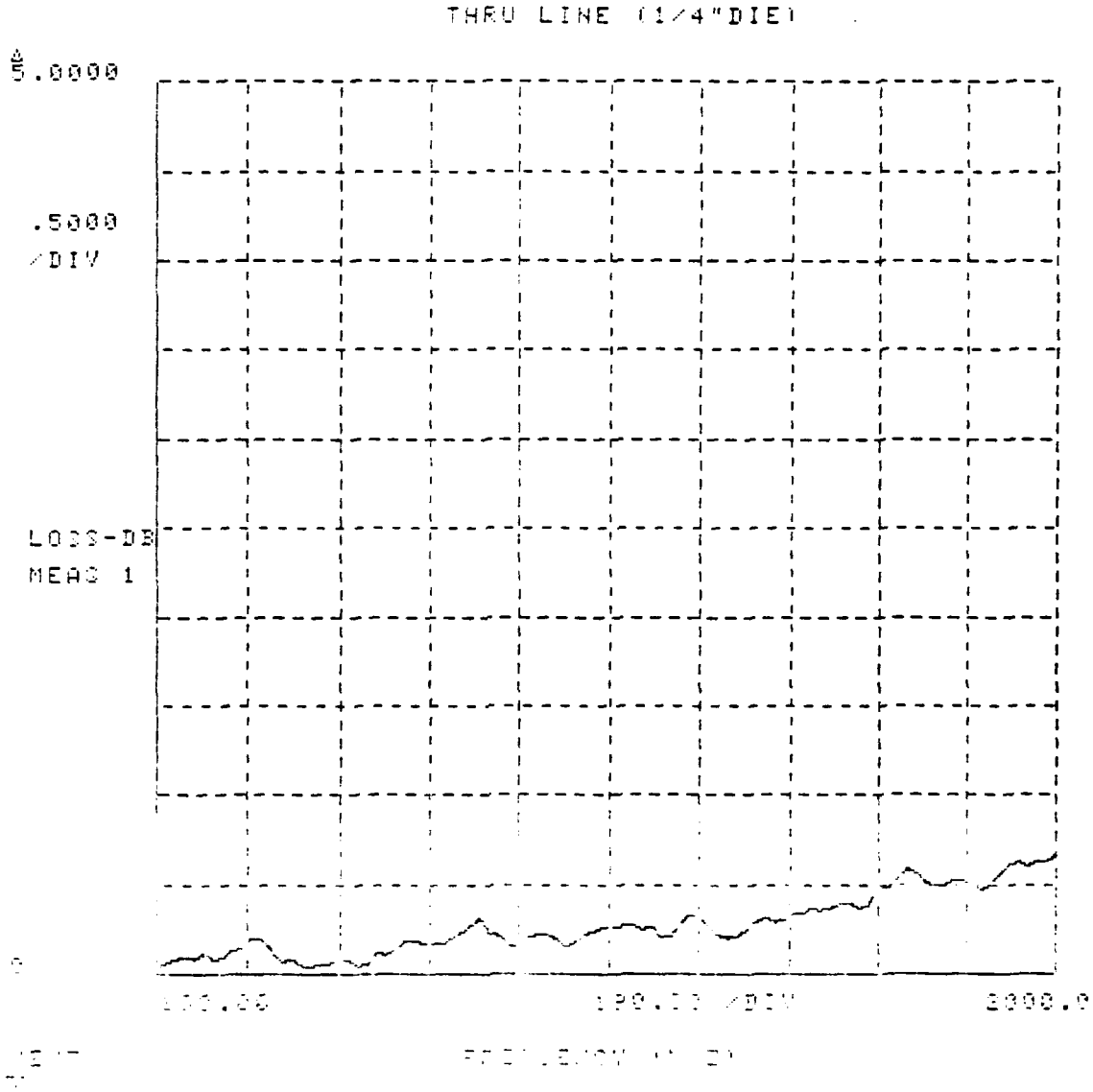

Fig. 9 — Measured insertion loss versus frequency for back-to-back N-type to microstrip (nominally 50-ohm) transitions on 1/4 inch thick k = 13 Stycast board.

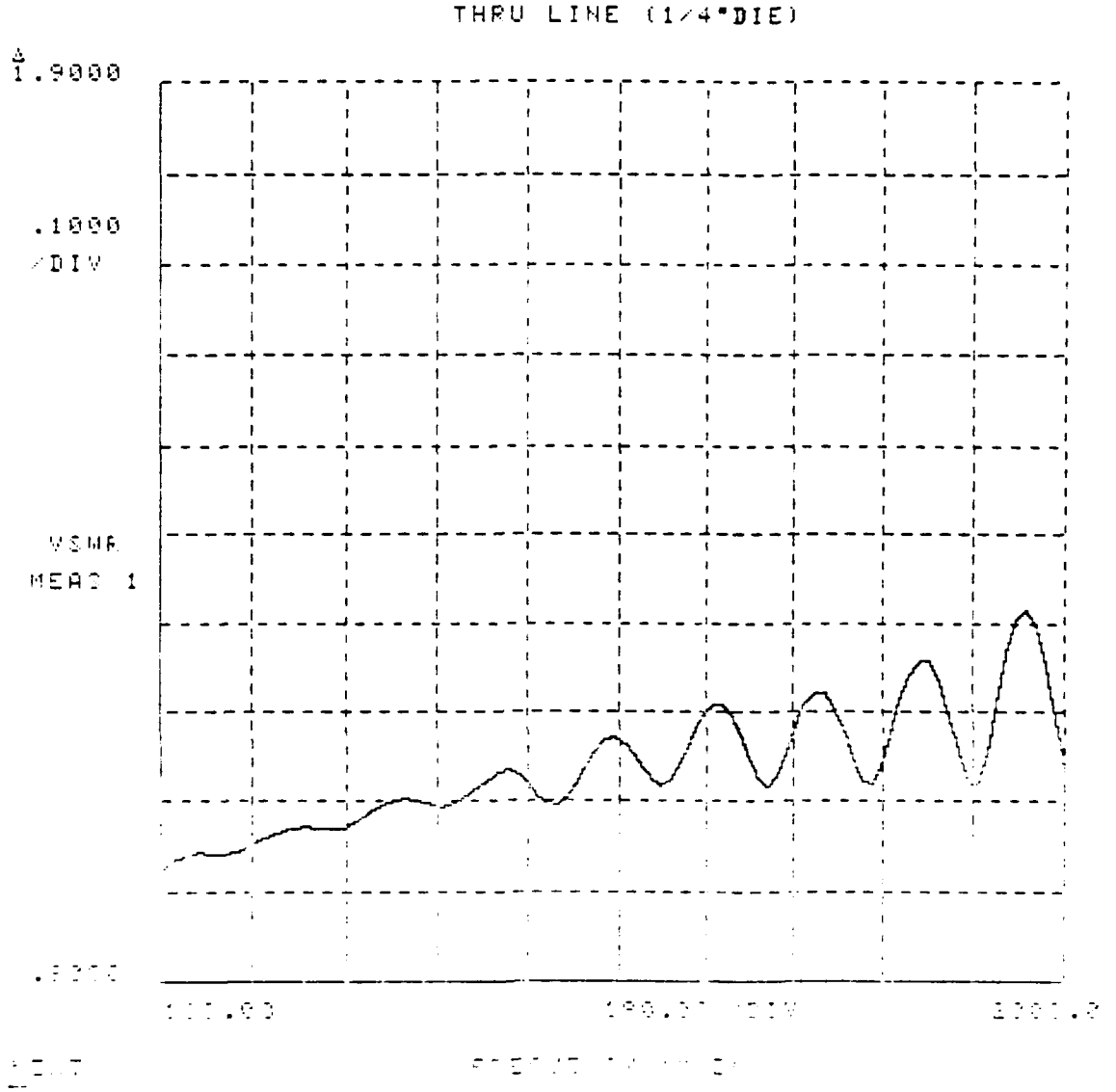

Fig. 10 — Measured VSWR versus frequency for back-to-back N-type to microstrip (nominally 50-ohm) transitions on 1/4 inch thick k = 13 Stycast board.

References

1. Plourde, J. K. and C. L. Ren, "Application of Dielectric Resonators in Microwave Components," IEEE Trans. Micr. Th. Techs., Vol. MTT-29, No. 8, August 1981, pp. 754-70.

2. Stiglitz, M. R., "Dielectric Resonators: Past, Present, Future," Microwave Journal, Vol. 24, No. 7, July 1981, p. 19.

3. Bastida, E. M. and P. Bergamini, "GaAs Monolithic Circuits Mounted over High Q Dielectric Resonators," IEEE 1982 Micr. and Mm-Wave Mono. Ckts. Symp. Digest of Papers, Dallas, TX, June 18, 1982, pp. 1115.

4. Dydyk, M., "Apply High-Q Resonators to MM-Wave Microstrip," Microwaves, Vol. 19, No. 13, December 1980, pp. 62-3.

5. Dydyk, M., "Dielectric Resonators Add Q to MIC Filters," Microwaves, Vol. 16, No. 12, December 1977, pp. 150-60.

6. Oliner, A. A. and L. Goldstone, "Leaky-Wave Antennas," IRE Trans., Vol. AP-7, October 1959, p. 307.

END

DATE
FILMED

10 — 83

DTIC